AIMS Materials Science, 10(3): 426–436.
DOI: 10.3934/matersci.2023023
Received: 25 November 2022
Revised: 24 March 2023
Accepted: 10 April 2023
Published: 08 May 2023

http://www.aimspress.com/journal/Materials

Research article

Effect of the calcination temperature of the FTO/PbS cathode on the performance of a quantum dot-sensitized solar cell

Ha Thanh Tung[1], Ho Kim Dan[2,3,*] and Dang Huu Phuc[4]

[1] Faculty of Basic Sciences, Vinh Long University of Technology Education, Vinh Long city, Vietnam
[2] Optical Materials Research Group, Science and Technology Advanced Institute, Van Lang University, Ho Chi Minh City, Vietnam
[3] Faculty of Applied Technology, School of Technology, Van Lang University, Ho Chi Minh City, Vietnam
[4] Faculty of Fundamental Science, Industrial University of Ho Chi Minh City, No. 12 Nguyen Van Bao, Ward 4, Go Vap District, Ho Chi Minh City, 700000, Vietnam

* **Correspondence:** Email: hokimdan@vlu.edu.vn.

Abstract: As a cheaper alternative to the industrial Pt electrode used in quantum-sensitized solar cells, the electrophoresis process is employed to create the low-cost FTO/PbS cathode. For structural cubic and sizes ranging from 40 nm to 200 nm, structure and morphology were investigated using high-resolution scanning electron microscopy and X-ray diffraction. The conversion efficiency of solar cells is significantly impacted by the calcination temperatures of cathodes at 100 ℃, 150 ℃, 200 ℃, and 300 ℃ under vacuum. The FTO/PbS cathode electrode was therefore calcined at 150 ℃ with a maximum efficiency of 3.938%. This happens as a result of the complete fusion of PbS nanoparticles with crystal at 150 ℃, which reduces resistance and increases electron lifetime compared to other temperature combinations.

Keywords: cathode; PbS film; electrochemistry properties

1. Introduction

Inorganic semiconductor quantum dots (QDs), which produce electrons for use in solar cells and have highly powerful light absorption properties, were developed as such materials in recent years. CdS, CdSe, PbS, PbSe, and InP have all been used in quantum dot sensitized solar cells (QDSSCs) [1,2]. The QDs have several advantages over dye molecules, including the ability to modify the particle size to change the bandgap energy [3], a higher optical absorption coefficient than dye molecules [4], and the formation of many more exciton pairs when photons are absorbed. Currently, QDSSCs have a lower conversion efficiency than dye-sensitized solar cells (DSSCs) [5–9].

The amazing studies [9–11] are all carried out on single quantum dots, which hardly absorb sunlight and do not fully exploit the visible region. More specifically, the bulk materials' absorption wavelengths for CdS and CdSe are respectively 550 and 705 nm. Both absorption wavelengths are considerably shorter than the aforementioned values at the scale of the QDs. The performance improvement was rather slight when the binding linker was employed after that. Extending the peak of the absorption spectrum well into the visible region while lowering recombination and dark current are required to improve QDSSC performance. Numerous groups have investigated the issue of expanding the absorption ranger by co-quantum dots, and the yield is significantly higher than that of devices using single quantum dot [12–15].

The counter electrode (CE), which is essential to boosting the conversion energy of devices because it receives electrons from the external circuit via a redox process at the surface of the electrolyte and the CE, was the subject of research in addition to the photoanodic electrode. The CE must consequently have a large surface area, high conductivity, and high electrochemical activity in order for the electrolyte's redox reactions to occur more quickly and be chemically stable at a low cost [16].

In a quest to replace the traditional CE Pt, researchers have spent years looking for CEs that might accomplish the aforementioned objectives. The ability of metal sulfide compounds such Mo_2S [17], NiS [18], FeS [19], CuS [20], and Cu_2S [12] to satisfy the aforementioned criteria and replace CE Pt has been demonstrated by researchers. Compared to the other materials in this category, copper sulfide (CuS, Cu_2S) is used in more studies because it has a band gap energy of 1.1–1.4 eV, a high electrochemical activity, and is stable in a polysulfide electrolyte [21–23]. According to the duration, temperature, and environment, thin copper (brass) films with a thickness of several micrometers are immersed in a polysulfide electrolyte to produce either a CuS thin film or a Cu_2S thin film. The copper brass, however, will continue to degrade if immersed in the electrolyte for a long time. This will increase the resistance of the film and cause a drop in the fill factor and open circuit potential, which will reduce the efficiency of QDSSCs [21–23].

PbS, which has the most consistent electrochemical activity among the other materials, has been investigated, fabricated, and employed in QDSSCs with a high efficiency of 3% [24] by Tachan's group and colleagues. The results show the material's potential. However, PbS has not been studied using a variety of fabrication methods, nor has it been investigated how the crystallization temperature of PbS film affects the electrochemical properties of the electrode and the conversion efficiency of solar cells. An FTO/PbS electrode's production is influenced by a number of variables, including the ratio of precursors, temperature, and calcination environment. In the earlier article, we were able to successfully raise the precursor ratio. Therefore, in this publication, we focus on studying CE crystallization at the calcination temperature. Choosing the right annealing temperature

is crucial for good crystallization since the electrical resistance of the CEs electrode effects crystallization. With better crystallization, the resistance of the crystal decreases. This is also the justification behind our choice to research and develop FTO/PbS cathode electrodes for the production of solar cells using electrophoresis at varied temperatures.

2. Materials and methods

2.1. Materials

The substrate for the cathode electrode film is a thin sheet of FTO (fluorine-doped tin oxide), a conductor with a low resistance of roughly 7 Ω/cm^2. The two diameters of commercial TiO_2 paste—400 nm as a light reflector and 20 nm as a transmission layer—are employed for the anode electrode. A full solar cell is created by joining two electrodes together using Meltonix 1170-25 (Surlyn). Using $Na_2S_2O_3$ $5H_2O$ and $Pb(NO_3)_2$ purchased from Sigma's company in Germany, we perform current and potential density measurements, electrochemical impedance measurements, and use colloidal silver as the path of the front and back of the solar cell. All of the aforementioned compounds are 99.9% pure.

2.2. Fabricated processes

The photoanode electrode is fabricated according to the process described in the group's previously published paper [25].

Commercial conductive glass (FTO, TEC7, Dyesol) was cut into several plates with an area of 1.2 cm × 2 cm each. The FTO plate is drilled with 2 small holes, 1 mm in diameter, used for injecting electrolyte solution. These bases are treated as shown in Figure 1.

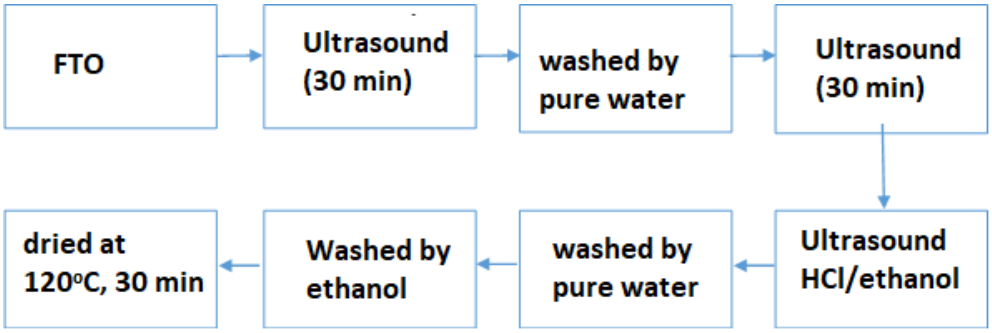

Figure 1. The diagram treatment of FTO.

The electrolyte solution used in this study is a polysulfide with an oxidation-reduction pair S^2/S_n^{2-} which was synthesized by dissolving 1.2 g of Na_2S with 0.064 g of sulfur powder and 0.149 g of KCl in 10 mL of aqueous methanol solution with a ratio of 7:3 to obtain a yellow color.

The cathode electrode of the PbS film was coated on the FTO conductive substrate by electrophoresis in a mixed solution of 2.0 mM $Pb(NO_3)_2$ and 1.0 mM NaS_2O_3 and dissolved in 100 mL of distilled water and methanol; adjust pH to 2.65. A voltage of 100 mV was used for 1 h for all samples; we fixed the concentration and pH and only changed the electrode heating temperature at

100 ℃, 150 ℃, 200 ℃, and 300 ℃ for 1 h in vacuum. Finally, we assemble the solar cell according to the structure from Figure 2.

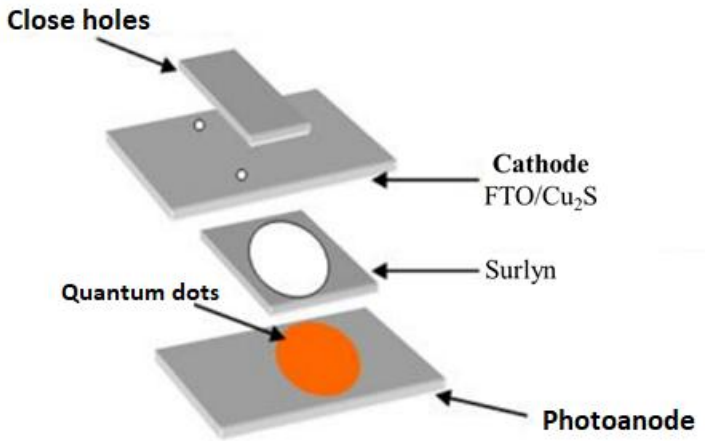

Figure 2. The structural QDSSCs completely.

2.3. Characterization

To study the properties of the cathode electrode, we used a high resolution surface scanning electromagnetic microscope at scanning potentials 15 kV and 1 kV (FESEM, SU820) for samples at different resolutions to analyze Geometric surface analysis of electrodes, Philips X-ray diffraction (XRD) spectroscopy, (PANalytical X'Pert) with CuKα radiation to determine the structure of PbS crystals on the FTO film, allowing size calculation particles and lattice parameters. After assembling the battery, we used the Keithley 2400 instrument and the SOLARENA sunlight simulation system to determine the current density and potential curves, thereby determining the conversion efficiency of the solar cells. Besides, in order to better understand the electron transfer processes through the cathode, we use electrochemical impedance spectroscopy to measure and determine the value of the resistances in the battery, including the resistances across the cathode surface with electrolyte to evaluate cathode activity.

3. Results and discussion

The FTO/PbS cathode electrode is depicted in high resolution scanning electron microscopy images in Figure 3 at various resolution levels. In general, the film's surface is quite porous, making it ideal for the electrode's electrochemical activity. The porous surface leaves a lot of empty spaces, making it easier for the polysulfide electrolyte solution to come into direct contact with the PbS nanoparticles and carry out the electrochemical reaction. The electrolyte system's electron exchange. The PbS nanoparticles were found to range in size from 40 nm to 200 nm, and they were extremely uniformly shaped like square or rectangular blocks. It is shown that the electrophoresis-created film is extremely stable.

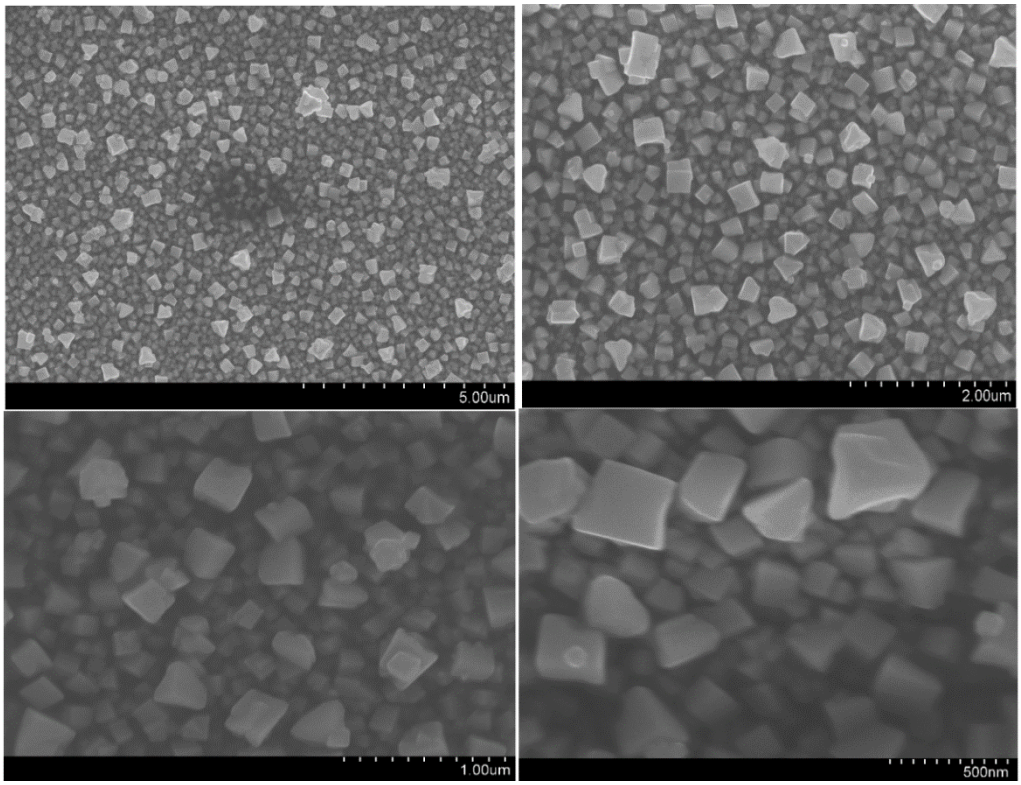

Figure 3. FESEM of FTO/PbS film was calcinted at 150 ℃ in vacuum environment with 500 nm, 1 μm, 2 μm and 5 μm resolution.

By using electrophoresis to create a strong adhesion film, the FTO/PbS electrode is created. To stop the formation of PbO, the film is crystallized in a vacuum. As a result, we first need to ascertain the structure of PbS in order to use it as electrodes. The FTO/PbS electrode's ray diffraction spectrum in a vacuum at 150 ℃ is shown in Figure 4, together with the PbS film's and the FTO substrate's distinctive diffraction peaks. The lattice planes with the Miller indices (111), (200), (220), (311), and (222) that correspond to the diffraction peaks at positions 26.1 º, 30.2 º, 43.19 º, 51.61 º, and 52.5 º fit well with the standard JCPDS card No. 05-0592 of the face-centered cubic structure. Additionally, this outcome is entirely consistent with the findings of the research groups Varma [26], Yang [27], and Shyju [28]. The PbS face-centered cubic's distinctive peak is the plane (200). We estimate the average particle size of the PbS at 150 ℃ to be about 48.9511 nm using Scherer's Eq 1 (see Table 1), which is in agreement with the findings of the FESEM pictures. Additionally, we noticed the characteristic peaks of the FTO conductive film at diffraction angles of 26.64 º, 33.85 º, and 37.9 º[29].

$$D = \frac{0.9\lambda}{\beta\cos\theta} \tag{1}$$

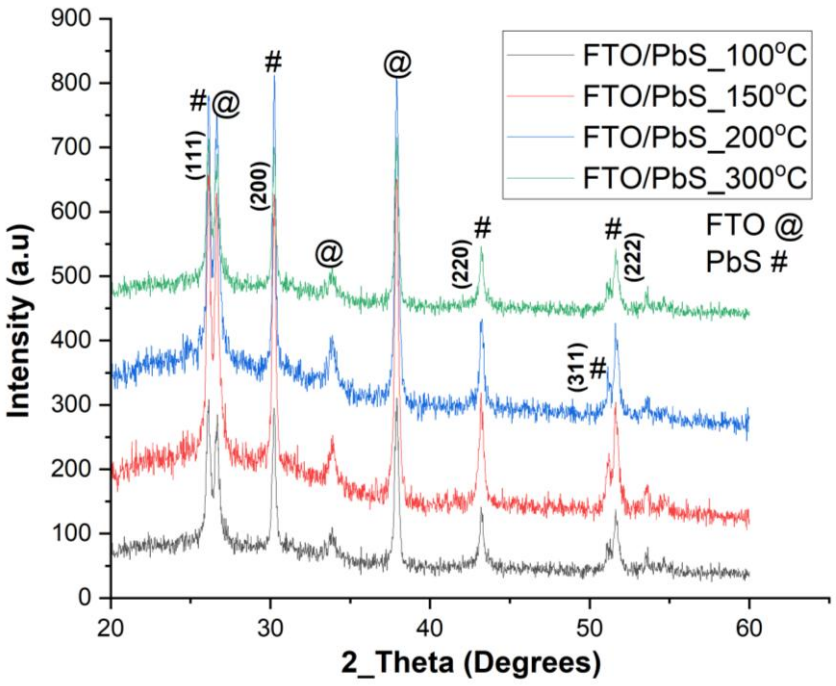

Figure 4. An XRD of FTO/PbS cathode was conducted at 100 ℃, 150 ℃, 200 ℃, and 300 ℃ in a vacuum environment for 1 h.

Where β is the half-width of the characteristic peak of PbS and D is the grain diameter.

Table 1. The structural parameters of the FTO/PbS cathode.

d-space (Å)	2θ (°)	(hkl)	D (nm)
3.4	26.1	(111)	48.9511
2.95	30.2	(200)	
2.09	43.19	(220)	
1.77	51.61	(311)	
2.74	52.5	(222)	

After examining the electrode's structural and morphological characteristics, we attach the cathode electrode and the anode using surlyn that has been heated to more than 100 ℃. The electrolyte is pumped and measured at the end. The parameters, short circuit current density (Jsc), open circuit potential (Voc), fill factor, and conversion efficiency of QDSSCs are determined using current and voltage density curves. Figure 5 displays the characteristic curves, and Table 2 displays the calculated values of the parameter. Figure 5 shows that the electrode heated to 150 ℃ has the highest current density (18.18 mA/cm^2) and the biggest open circuit voltage (0.572 V), resulting in a very high conversion efficiency of 3.938%. The conversion efficiency of this study is higher than that of studies by Tachan and co-workers (3%) and Zhang et al. (1.75%) [30], and it is in line with the findings of Yang and co-workers (3.91%) [27]. The achieved efficiency is substantially lower for the FTO/PbS cathode electrode heated at 100 ℃, 200 ℃, and 300 ℃, respectively: 2.579%, 1.929%, and 2.338%. As a result, it is clear that the temperature needed to create PbS crystals on the FTO substrate is crucial. This temperature has a significant impact on the electrochemical characteristics

of the cathode electrode, which in turn impacts the current density in cells and the functionality of QDSSCs.

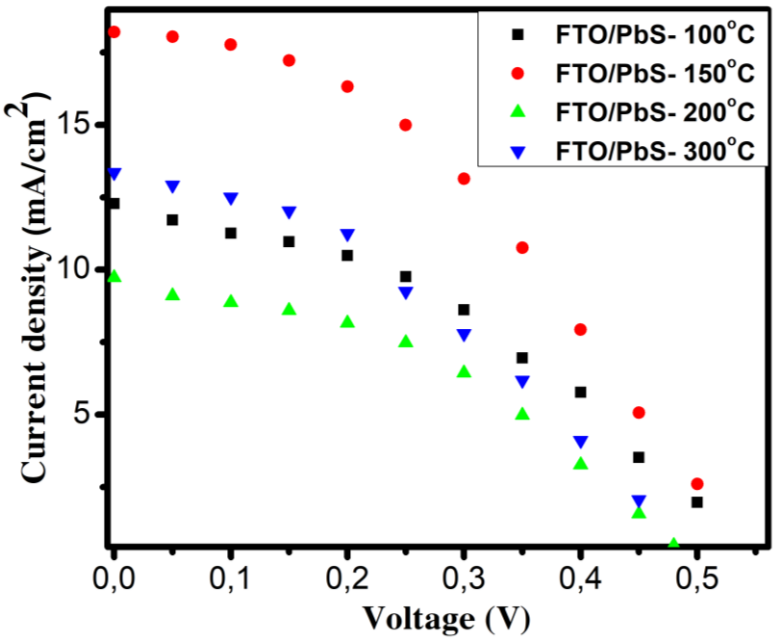

Figure 5. J-V cuvres of QDSSCs based on different cathodes.

Table 2. The electrochimical parameters of QDSSCs.

Electrodes	J_{SC} (mA/cm^2)	V_{OC} (V)	Fill factor (FF)	Efficiency (%)	R_{ct1} (Ω)	R_{ct2} (Ω)	τ_n (ms)
FTO/PbS-100 ℃	12.29	0.571	0.373	2.579	211.5	58.4	79.6
FTO/PbS-150 ℃	18.18	0.572	0.382	3.938	10.6	36.8	199
FTO/PbS-200 ℃	9.72	0.493	0.41	1.929	81.7	193	201.5
FTO/PbS-300 ℃	13.39	0.529	0.331	2.338	711.2	221	101.8

The speed of charge carriers in solar cells and the chemical composition of cathode electrodes are investigated using electrochemical impedance spectroscopy. We obtained the experimental EIS spectrum from the EIS spectrum in Figure 6 after measuring the solar cells, and we then used the specialized software Autolab to fit and calculate the resistance values of QDSSCs, such as: R_{ct1} is the resistance of the excited electrons that are transferred through the cathode and the cathode surface with polysulfide electrolyte, and R_{ct2} is the resistance of the excited electrons when moving through the photoanode to the external circuit. The EIS of QDSSCs, which were created using cathode electrodes heated at various temperatures in a vacuum atmosphere, is shown in Figure 6. Figure 6 illustrates this relationship between semi-circle size and resistance values; the cathode heated to 150 ℃ has the lowest Rct1 resistance (10.6 Ω), followed by cathodes heated to 100 ℃ (211 Ω), 200 ℃ (81.7 Ω), and 300 ℃ (711.2 Ω). This outcome can be explained by the fact that PbS layer on FTO crystallized more precisely at 150 ℃ than it did at higher heating temperatures. Additionally, all of the films were calcined in a vacuum to prevent Pb from oxidizing and becoming PbO. The outcomes of the XRD demonstrate this. Therefore, it can be said that the electrons moving through

the PbS film and across its surface with the S^{2-}/S_n^{2-} electrolyte do so at a faster rate the smaller the resistance value of R_{ct1}. The efficiency of the cells for the cathode heated at 150 ℃ is the highest due to its highest current density, and this result is entirely consistent with the results of the current and potential curve measurements of QDSSCs. This result is also entirely consistent with the findings of Zhang et al., who examined the PbS electrode film formation time [26] and compared it to that of the Pt electrode [30].

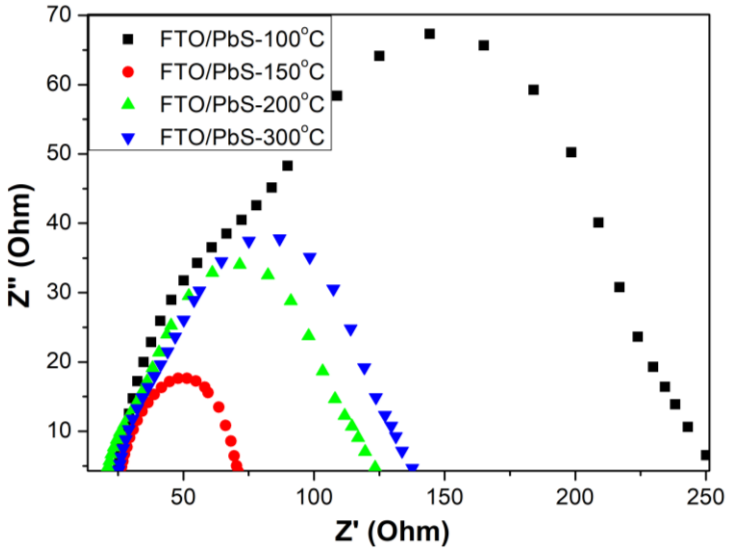

Figure 6. EIS of QDSSCs based on different cathodes.

The bode spectrum, which is depicted in Figure 7, is derived from electrochemical impedance spectroscopy and is used to determine how well excited electrons may recombine and how long electrons in the PbS film's conduction band live. The calculation results for electrodes heated at 100 ℃, 150 ℃, 200 ℃, and 300 ℃ for 1 h in a vacuum atmosphere are shown in Table 2. This is related to the minimum frequency by the formula $\tau_{max} = \frac{1}{2\pi f_{min}}$. According to Table 2, when two cathode electrodes are heated to 150 ℃, the lifetime of QDSSCs is the longest (199 ms and 201.5 ms) at 200 ℃, and it is subsequently half at 300 ℃ (101.8 ms). The electrode is heated to 100 ℃ for a brief period of time (79.6 ms) since PbS crystals didn't crystallize perfectly. The measured current density is larger than that of other electrodes because the longer the lifespan, the less likely it is that the electron will recombine with the hole in the material's valence band. This result is in perfect accordance with the findings of current and potential density (J-V) curve measurements as well as X-ray diffraction (PbS crystals crystallize most efficiently at 150 ℃).

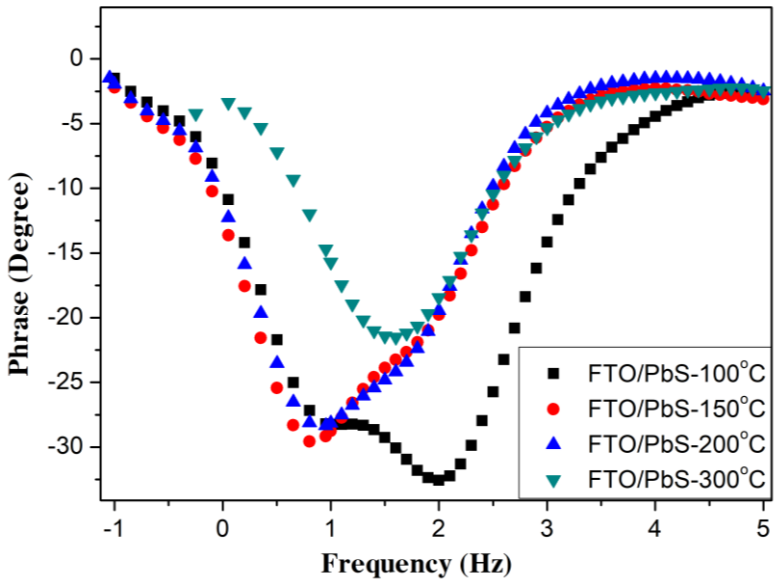

Figure 7. Bode plots of QDSSCs with different cathodes**.**

4. Conclusions

Electrophoresis is used to create the FTO/PbS cathode electrode at a voltage of 100 mV, which changes depending on the calcination temperature. Due to its reduced cost and superior performance, the film is utilized to replace commercial Pt electrodes. The PbS nanofilm was effectively created on the FTO conductive substrate as a result, and it possesses a face-centered cubic structure, excellent crystallinity, and somewhat uniform particle size, according to FESEM and XRD. We note the highest current density and efficiency performance at 18.18 mA/cm^2 and 3.938% with an FTO/PbS cathode electrode at 150 ℃ when compared to other heating temperatures based on the findings of measuring current density and potential. What's more, this outcome was better than that of other research teams. The electrochemical impedance spectrum, commonly known as the bode spectrum, can also be used to explain the performance's outcomes. According to the findings, the PbS film was calcined at 150 ℃ for flawless crystallization, which resulted in fewer crystal lattice defects and recombination processes, as well as the least R_{ct1} resistance (10.6 Ω) and the longest lifetime (199 ms).

Conflict of interest

The authors declare that they have no conflict of interest.

References

1. Zaban AMOI, Mićić OI, Gregg BA, et al. (1998) Photosensitization of nanoporous TiO_2 electrodes with InP quantum dots. *Langmuir* 14: 3153–3156. https://doi.org/10.1021/la9713863
2. Yu P, Zhu K, Norman AG, et al. (2006) Nanocrystalline TiO_2 solar cells sensitized with InAs quantum dots. *J Phys Chem B* 110: 25451–25454. https://doi.org/10.1021/jp064817b

3. Yu WW, Wang YA, Peng X (2003) Formation and stability of size-, shape-, and structure-controlled CdTe nanocrystals: ligand effects on monomers and nanocrystals. *Chem Mater* 15: 4300–4308. https://doi.org/10.1021/cm034729t
4. Beard MC (2011) Multiple exciton generation in semiconductor quantum dots. *J Phys Chem Lett* 2: 1282–1288. https://doi.org/10.1021/jz200166y
5. Fang J, Wu J, Lu X, et al. (1997) Sensitization of nanocrystalline TiO_2 electrode with quantum sized CdSe and ZnTCPc molecules. *Chem Phys Lett* 270: 145-151. https://doi.org/10.1016/S0009-2614(97)00333-3
6. Lee W, Kwak WC, Min SK, et al. (2008) Spectral broadening in quantum dots-sensitized photoelectrochemical solar cells based on CdSe and Mg-doped CdSe nanocrystals. *Electrochem Commun* 10: 1699–1702. https://doi.org/10.1016/j.elecom.2008.08.025
7. Liu D, Kamat PV (1993) Photoelectrochemical behavior of thin cadmium selenide and coupled titania/cadmium selenide semiconductor films. *J Physical Chemistry* 97: 10769-10773. https://doi.org/10.1021/j100143a041
8. Peter LM, Riley DJ, Tull EJ, et al. (2002) Photosensitization of nanocrystalline TiO_2 by self-assembled layers of CdS quantum dots. *Chem Commun* 10: 1030–1031. https://doi.org/10.1039/b201661c
9. Vogel R, Pohl K, Weller H (1990) Sensitization of highly porous, polycrystalline TiO_2 electrodes by quantum sized CdS. *Chem Phys Lett* 174: 241–246. https://doi.org/10.1016/0009-2614(90)85339-E
10. Mora-Seró I, Giménez S, Moehl T, et al. (2008) Factors determining the photovoltaic performance of a CdSe quantum dot sensitized solar cell: the role of the linker molecule and of the counter electrode. *Nanotechnology* 19: 424007. https://doi.org/10.1088/0957-4484/19/42/424007
11. Shen YJ, Lee YL (2008) Assembly of CdS quantum dots onto mesoscopic TiO_2 films for quantum dot-sensitized solar cell applications. *Nanotechnology* 19: 045602. https://doi.org/10.1088/0957-4484/19/04/045602
12. Lee YL, Lo YS (2009) Highly efficient quantum-dot-sensitized solar cell based on co-sensitization of CdS/CdSe. *Adv Funct Mater* 19: 604–609. https://doi.org/10.1002/adfm.200800940
13. Zhang Q, Zhang Y, Huang S, et al. (2010) Application of carbon counterelectrode on CdS quantum dot-sensitized solar cells (QDSSCs). *Electrochem Commun* 12: 327–330. https://doi.org/10.1016/j.elecom.2009.12.032
14. Sudhagar P, Jung JH, Park S, et al. (2009) The performance of coupled (CdS: CdSe) quantum dot-sensitized TiO_2 nanofibrous solar cells. *Electrochem Commun* 11: 2220–2224. https://doi.org/10.1016/j.elecom.2009.09.035
15. Yu Z, Zhang Q, Qin D, et al. (2010) Highly efficient quasi-solid-state quantum-dot-sensitized solar cell based on hydrogel electrolytes. *Electrochem Commun* 12: 1776–1779. https://doi.org/10.1016/j.elecom.2010.10.022
16. Wang S, Tian J (2016) Recent advances in counter electrodes of quantum dot-sensitized solar cells. *RSC Adv* 6: 90082–90099. https://doi.org/10.1039/C6RA19226B
17. Kamaja CK, Devarapalli RR, Dave Y, et al. (2016) Synthesis of novel Cu_2S nanohusks as high performance counter electrode for CdS/CdSe sensitized solar cell. *J Power Sources* 315: 277–283. https://doi.org/10.1016/j.jpowsour.2016.03.027

18. Kim HJ, Kim DJ, Rao SS, et al. (2014) Highly efficient solution processed nanorice structured NiS counter electrode for quantum dot sensitized solar cells. *Electrochim Acta* 127: 427–432. https://doi.org/10.1016/j.electacta.2014.02.019
19. Chen H, Zhu L, Liu H, et al. (2014) Efficient iron sulfide counter electrode for quantum dots-sensitized solar cells. *J Power Sources* 245: 406–410. https://doi.org/10.1016/j.jpowsour.2013.06.004
20. Raj CJ, Prabakar K, Savariraj AD, et al. (2013) Surface reinforced platinum counter electrode for quantum dots sensitized solar cells. *Electrochim Acta* 103: 231–236. https://doi.org/10.1016/j.electacta.2013.04.016
21. Selopal GS, Zhao H, Tong X, et al. (2017) Highly stable colloidal "giant" quantum dots sensitized solar cells. *Adv Funct Mater* 27: 1701468. https://doi.org/10.1002/adfm.201701468
22. Jiao S, Shen Q, Mora-Sero I, et al. (2015) Band engineering in core/shell ZnTe/CdSe for photovoltage and efficiency enhancement in exciplex quantum dot sensitized solar cells. *ACS Nano* 9: 908–915. https://doi.org/10.1021/nn506638n
23. Kim JY, Yang J, Yu JH, et al. (2015) Highly efficient copper-indium-selenide quantum dot solar cells: suppression of carrier recombination by controlled ZnS overlayers. *ACS Nano* 9: 11286–11295. https://doi.org/10.1021/acsnano.5b04917
24. Tachan Z, Shalom M, Hod I, et al. (2011) PbS as a highly catalytic counter electrode for polysulfide-based quantum dot solar cells. *J Phys Chem C* 115: 6162–6166. https://doi.org/10.1021/jp112010m
25. Nguyen TP, Ha TT, Nguyen TT, et al. (2018) Effect of Cu^{2+} ions doped on the photovoltaic features of CdSe quantum dot sensitized solar cells. *Electrochim Acta* 282: 16–23. https://doi.org/10.1016/j.electacta.2018.06.046
26. Thulasi-Varma CV, Rao SS, Ikkurthi KD, et al. (2015) Enhanced photovoltaic performance and morphological control of the PbS counter electrode grown on functionalized self-assembled nanocrystals for quantum-dot sensitized solar cells via cost-effective chemical bath deposition. *J Mater Chem C* 3: 10195–10206. https://doi.org/10.1039/C5TC01988E
27. Yang Y, Zhu L, Sun H, et al. (2012) Composite counter electrode based on nanoparticulate PbS and carbon black: towards quantum dot-sensitized solar cells with both high efficiency and stability. *ACS Appl Mater Interfaces* 4: 6162–6168. https://doi.org/10.1021/am301787q
28. Shyju TS, Anandhi S, Sivakumar R, et al. (2014) Studies on lead sulfide (pbs) semiconducting thin films deposited from nanoparticles and its nlo application. *Int J Nanosci* 13: 1450001. https://doi.org/10.1142/S0219581X1450001X
29. Turgut G, Koçyiğit A, Sönmez E (2015) Influences of Pr and Ta doping concentration on the characteristic features of FTO thin film deposited by spray pyrolysis. *Chinese Phys B* 24: 107301. https://doi.org/10.1088/1674-1056/24/10/107301
30. Zhang JB, Zhao FY, Tang GS, et al. (2013) Influence of highly efficient PbS counter electrode on photovoltaic performance of CdSe quantum dots-sensitized solar cells. *J Solid State Electr* 17: 2909–2915. https://doi.org/10.1007/s10008-013-2210-4

AIMS Press